Available online at www.sciencedirect.com

ScienceDirect

Procedia Manufacturing 10 (2017) 351 – 362

Procedia MANUFACTURING

45th SME North American Manufacturing Research Conference, NAMRC 45, LA, USA

Amplitude Ratio: A New Metric for Milling Stability Identification

Mark A. Rubeo* and Tony L. Schmitz

The University of North Carolina at Charlotte, Charlotte, NC, 28223, USA

Abstract

This paper describes a metric referred to as the "amplitude ratio" for evaluating the stability of milling operations via time domain simulation. The amplitude ratio is used to generate contour diagrams that identify stability behavior over a range of spindle speeds and axial depths of cut. The suitability of the amplitude ratio stability metric is evaluated through comparison to independently published results obtained using semi-analytical techniques.

Peer-review under responsibility of the organizing committee of the 45th SME North American Manufacturing Research Conference

Keywords: Milling, stability, chatter, simulation

1. Introduction

The study of machining vibrations can be traced back to the early 1900s. In work published by Taylor [1] the challenges presented by chatter are noted as the "most obscure and delicate of all problems facing the machinist." However, it wasn't until the 1950s and 1960s that the primary mechanism of chatter was revealed by Tobias, Tlusty, and Merritt [2-4]. Their research revealed regeneration of surface waviness (or the regenerative effect) as a primary chatter mechanism. This discovery led to the development of analytical models for predicting the occurrence of chatter using stability lobe diagrams, which separate the domain of spindle speed and axial depth of cut into stable and unstable regions. Since that time numerous researchers have used analytical, semi-analytical, and numerical models to predict stability behavior in milling. In many cases, chatter is the critical factor influencing milling productivity and the technical challenge of chatter prediction motivates continuing research efforts.

Time domain simulation is a powerful tool for studying machining stability. Each iteration of the simulation results in "local" information (i.e., specific to an individual set of machining process parameters) such as

* Corresponding author. Tel.: +1-704-687-5086
E-mail address: mrubeo@uncc.edu

Peer-review under responsibility of the organizing committee of the 45th SME North American Manufacturing Research Conference
doi:10.1016/j.promfg.2017.07.004

accelerations, velocities, and displacements of the cutting tool and workpiece. Researchers have used this "local" information to develop stability metrics for evaluating "global" stability behavior over a range of spindle speeds and axial depths of cut similar to the traditional stability lobe diagram. In [5] Smith and Tlusty use peak-to-peak cutting forces to generate contour maps. These contour maps, referred to as peak-to-peak force diagrams, indicate stability by the rate of change of cutting forces over the spindle speed-axial depth of cut domain. Campomanes and Altintas use the actual trochoidal tooth path to improve the simulation of low radial immersion milling. Chatter detection is facilitated by calculating a "nondimensional chatter coefficient" which is the ratio of the maximum uncut chip thickness during a time domain simulation with flexible dynamics and the maximum uncut chip thickness during a time domain simulation with rigid dynamics [6]. In [7] Honeycutt and Schmitz develop a stability metric based on the once-per-tooth sampled displacement of the cutting tool. The absolute value of the difference in the successive sampled points is summed. If the cut is stable (forced vibrations), the sampled points repeat and the stability metric value is nominally zero. Otherwise the sampled points do not repeat and the stability metric is greater than zero.

In this paper, a new stability metric, which will be referred to as the "amplitude ratio," is presented. The time domain simulation model is described which includes a mechanistic force model and Eulerian integration approach for solving the dynamic equations of motion. The suitability of the amplitude ratio is evaluated through comparison with independently published results. The conclusions summarize the usefulness of the new metric.

Nomenclature

$h(t)$	instantaneous, uncut chip thickness
f_t	feed per tooth
τ	tooth passing period
$n(t)$	relative vibration between the tool and workpiece in the instantaneous surface normal direction for the current cutting tooth
$n(t-\tau)$	relative vibration between the tool and workpiece in the instantaneous surface normal direction for the previous cutting tooth
r	cutting tooth specific runout
x_t	tool vibration in the *x* direction
y_t	tool vibration in the *y* direction
x_w	workpiece vibration in the *x* direction
y_w	workpiece vibration in the *y* direction
φ	cutter rotation angle
F_t	instantaneous tangential cutting force
F_r	instantaneous radial cutting force
F_a	instantaneous axial cutting force
K_{tc}	specific cutting force coefficient in the tangential direction
K_{rc}	specific cutting force coefficient in the radial direction
K_{ac}	specific cutting force coefficient in the axial direction
K_{te}	edge force coefficient in the tangential direction
K_{re}	edge force coefficient in the radial direction
K_{ae}	edge force coefficient in the axial direction
C_t	process damping coefficient in the tangential direction
C_r	process damping coefficient in the radial direction
b	chip width (axial depth of cut)
$\dot{r}$	velocity in the radial direction
V	cutting speed
m_q	modal mass
c_q	modal damping
k_q	modal stiffness
Δt	time step
$\ddot{q}$	modal acceleration

$\dot{q}$	modal velocity
q	modal displacement
r_{amp}	amplitude ratio
A_{cf}	amplitude of the chatter frequency component
A_{tpf}	amplitude of the tooth passing frequency component
p	helical pitch
D	tool diameter
N	number of cutting teeth
η	helix angle

2. Time Domain Simulation Model

The time domain simulation, which is based on the "regenerative force, dynamic deflection model" described in [5, 8-10], numerically solves the governing equations of motion for milling at small, incremental time steps. At each incremental time step the time domain simulation performs three core functions:

1. the instantaneous, uncut chip thickness is calculated
2. the instantaneous cutting forces are calculated
3. the governing equations of motion are solved.

The time domain simulation is able to account for nonlinearities that occur during the milling process, such as the case where deflection of the tool/workpiece become large enough that contact is lost [11], and the case of highly interrupted cutting during low radial immersion milling [12]. The simulation model includes the assumptions that the path of each milling tooth can be approximated as a circle and that the cutting forces are proportional to the uncut chip area.

The instantaneous, uncut chip thickness depends on the commanded feed per tooth, the vibration of the tool and workpiece for the current and previous cutting teeth, and flute-to-flute runout of the cutting tool. Therefore, instantaneous chip thickness is expressed as:

$$h(t) = f_t \sin(\varphi) + n(t-\tau) - n(t) + r \tag{1}$$

where $f_t \sin(\varphi)$ is the nominal, tooth angle-dependent chip thickness, $n(t-\tau)$ is the relative vibration between the tool and workpiece in the direction of the instantaneous surface normal for the previous cutting tooth, $n(t)$ is the relative vibration between the tool and workpiece in the instantaneous surface normal direction for the current cutting tooth, and r is the cutting tooth specific runout. In these expressions, f_t is the feed per tooth, φ is the cutter rotation angle, t is the current time, and τ is the tooth passing period. The vibrations in the direction of the surface normal depend on the relative vibrations between the tool and workpiece in the x and y directions as well as the cutter rotation angle and may be expressed as:

$$n(t) = -(x_t - x_w)\sin(\varphi) - (y_t - y_w)\cos(\varphi) \tag{2}$$

where x_t and y_t are the tool vibrations and x_w and y_w are the workpiece vibrations.

Cutting force calculations are based on the mechanistic force model presented by Budak, Altintas, and Armarego in [13] and augmented with the process damping force presented by Tyler and Schmitz in [14]. At each incremental time step, the chip thickness is evaluated and, in the case where the tool has vibrated out of the cut (i.e., the instantaneous, uncut chip thickness is found to be less than or equal to zero), the instantaneous tangential, radial, and axial cutting forces are set to zero. For the case where the instantaneous, uncut chip thickness is greater than zero, the instantaneous tangential, radial, and axial cutting forces can be expressed, respectively, as:

$$F_t^{i+1} = K_{tc} b h^{i+1} + K_{te} b - C_t b \frac{\dot{r}^i}{V} \tag{3}$$

$$F_r^{i+1} = K_{rc} b h^{i+1} + K_{re} b - C_r b \frac{\dot{r}^i}{V} \tag{4}$$

$$F_a^{i+1} = K_{ac} b h^{i+1} + K_{ae} b \tag{5}$$

where b is the axial depth of cut and h^{i+1} is the instantaneous, uncut chip thickness for the current time step. K_{tc}, K_{rc}, and K_{ac} are the tangential, radial, and axial specific cutting force coefficients, respectively, which are associated with the "cutting" or shearing taking place during chip formation. The tangential, radial, and axial edge force coefficients, K_{te}, K_{re}, and K_{ae}, capture the ploughing effect which occurs at small chip thicknesses. The expressions $C_t b \dot{r}^i/V$ and $C_r b \dot{r}^i/V$ are the process damping forces in the tangential and radial directions, respectively, where C_t and C_r are the tangential and radial process damping coefficients, $\dot{r}^i$ is the velocity in the radial direction calculated in the previous time step, and V is the cutting speed [14]. These instantaneous cutting forces are then transformed into the coordinate system shown in Fig. 1.

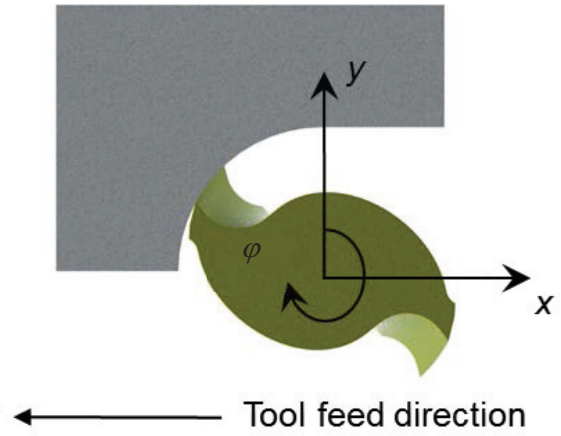

Fig. 1. Coordinate system definition for the time domain simulation model. A down milling configuration is shown.

The equations of motion are solved numerically in modal coordinates using an Euler integration, or "time-marching", scheme. The dynamics of the tool and workpiece are represented using modal parameters for an arbitrary number of degrees of freedom. The tool dynamics are considered in two orthogonal directions in the plane of the cut and the workpiece dynamics are considered in all three orthogonal directions. In modal coordinates the dynamic equation of motion may be expressed as:

$$F_q^i = m_q \ddot{q}^i + c_q \dot{q}^i + k_q q^i \tag{6}$$

Then, as an approximated solution for velocity, $\dot{q}^{i+1}$, and displacement, q^{i+1}, via Euler integration:

$$\ddot{q}^{i+1} = \frac{\left(F_q^i - c_q \dot{q}^i - k_q q^i\right)}{m_q} \tag{7}$$

$$\dot{q}^{i+1} = \dot{q}_i + \ddot{q}^{i+1}\Delta t \tag{8}$$

$$q^{i+1} = q^i + \dot{q}^{i+1}\Delta t \tag{9}$$

where m_q, c_q, and k_q are the mass, damping, and stiffness values, respectively, expressed in modal coordinates, and Δt is the time step.

Additionally, the simulation model allows for a variety of tool geometries including an arbitrary number of cutting teeth, variable teeth spacing, different helix angles for each tooth, and cutter teeth runout. As a practical consideration it is important to select a time step which is sufficiently small that the Euler integration method provides a numerically stable solution. A rule of thumb is that the time step should be at least ten times smaller than the period associated with the highest oscillation frequency present in the system being modeled. Also, the number of time steps (i.e., cutting tool revolutions) should be sufficiently high for the initial transient behavior to decay.

The outcome of individual time domain simulations contains "local" information specific to the individual spindle speed-axial depth of cut combinations. This includes the instantaneous cutting forces and tool/workpiece deflections, velocities, and accelerations. In order to extend the utility of the time domain simulation to predict "global" milling stability information over a range of spindle speeds and axial depths of cut, a suitable stability metric is required. The stability metric is calculated for each combination of spindle speed and axial depth of cut over a user-specified range and used to generate a contour map. In this paper, the authors propose the amplitude ratio as a suitable stability metric and demonstrate its suitability by comparison to published results.

3. Amplitude Ratio Diagram

In an effort to establish a distinct boundary between stable and unstable machining behavior using time domain simulation, a new stability metric has been developed. The amplitude ratio stability metric provides a quantitative measure of the existence and severity of chatter.

As previously mentioned, the outcome of individual time domain simulations contains "local" information specific to the individual spindle speed-axial depth of cut combinations. This includes the instantaneous cutting forces and tool/workpiece deflections, velocities, and accelerations which can be represented in the frequency domain. For an individual time domain simulation of a stable machining operation, the frequency content of the milling signals contains the tooth passing frequency, runout frequency, and their multiples (or harmonics). Therefore, stable cuts may be described as having a "clean" sound. Unstable cuts also contain these frequency components, however, they also exhibit a chatter frequency which results in a "harsh" sound on the shop floor. This chatter frequency is typically close to the natural frequency of the most flexible structure in the machine-tool-workpiece system. Since chatter (i.e., secondary Hopf instability) can be recognized by the manifestation of a chatter frequency, the severity of chatter can be established by the amplitude of the chatter frequency component relative to the amplitude of the tooth passing frequency component.

Amplitude ratio diagrams are generated through multiple iterations of a time domain simulation over the desired range of spindle speed and axial depth of cut combinations. At the conclusion of each simulation the steady state portion of a frequency domain milling signal is examined for the maximum amplitude of the tooth passing frequency (and harmonics) component and, if present, the chatter frequency component. Fig. 2 provides an illustrative example where the selected milling signal is the relative displacement between the tool and workpiece. For the purposes of experimental validation, a measurable quantity, such as workpiece velocity (laser vibrometer) or acceleration (accelerometer), may be selected.

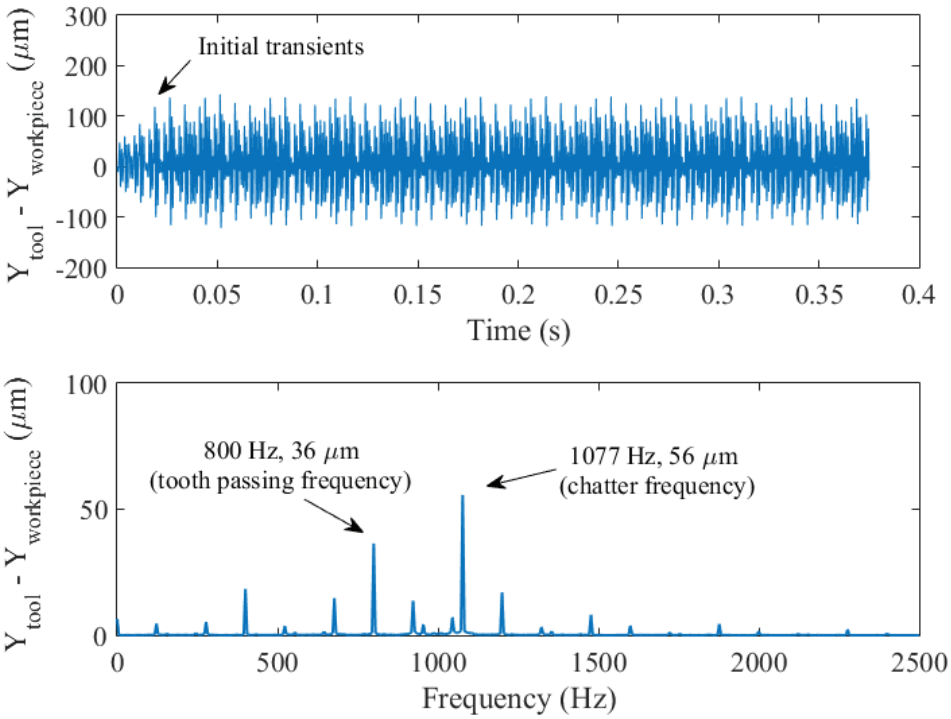

Fig. 2. The relative displacement of the tool and workpiece given in the time (top) and frequency (bottom) domains. The tooth passing frequency component and chatter frequency component are indicated in the bottom panel and the amplitude ratio is calculated as 56/36 = 1.56.

Finally the amplitude ratios for each combination of spindle speed and axial depth of cut are plotted as a contour map. The amplitude ratio, r_{amp}, is calculated as:

$$r_{amp} = \frac{A_{cf}}{A_{tpf}} \tag{10}$$

where A_{cf} is the amplitude of the chatter frequency component and A_{tpf} is the maximum amplitude of the tooth passing frequency (and harmonics) component in a given milling signal. An illustrative example of an amplitude ratio diagram is displayed in Fig. 3. This diagrams provide global stability information over a range of spindle speeds and axial depths of cut. Large stable regions (white) are evident that are predicted to contain no chatter frequency component. Further, the severity of chatter is evident by value of the amplitude ratio. It may be the case that a small chatter frequency component ($r_{amp} \ll 1$) is acceptable for most machine shop applications. However, as the amplitude ratio becomes larger chatter becomes increasingly severe.

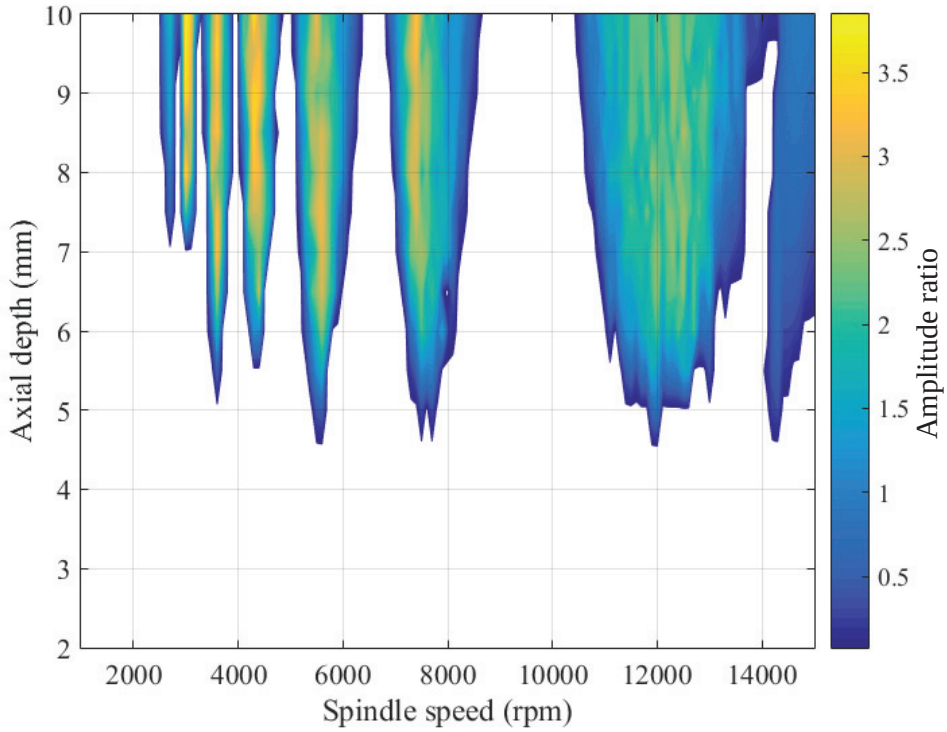

Fig. 3. Example amplitude ratio diagram.

4. Results

To evaluate the amplitude ratio diagrams, comparison to results found in the literature are presented. Two cases of interest in milling have been selected for the study: (1) period-2 (or flip) instability [15] and (2) helix angle induced islands of instability [16]. Both cases occur during low radial immersion milling.

4.1. Period-n Flip Instability

In [15] Govekar *et al.* use the semi-discretization method to identify secondary Hopf and period-2 instabilities during low radial immersion milling. A single flute, 8 mm diameter endmill clamped in an HSK40E shrink fit holder with a 96 mm overhang and 45° helix angle was used for the up milling tests. The 5% radial immersion (i.e., 0.4 mm radial depth of cut) provided highly interrupted (i.e., low radial immersion) cutting conditions. The specific cutting force and force angle for the aluminum workpiece-tool combination was determined mechanistically to be 644 MPa and 69.7°,, respectively. The stability diagram, shown in Fig. 4, was experimentally verified.

The large length-to-diameter ratio of the cutting tool resulted in a single, dominant vibration mode for which the modal parameters in the *x* (feed) and *y* directions are given in Table 1. The stability diagram obtained using the semi-discretization approach is displayed in Fig. 4. It shows that the Hopf instabilities are open curves distributed along the spindle speed axis and the period-2 instabilities manifest as close curves.

Table 1. Cutting tool modal parameters obtained from impact testing.

x (feed) direction		
f_n (Hz)	k (N/m)	ζ
721	4.1×10^5	0.009
y direction		
f_n (Hz)	k (N/m)	ζ
721	4.1×10^5	0.009

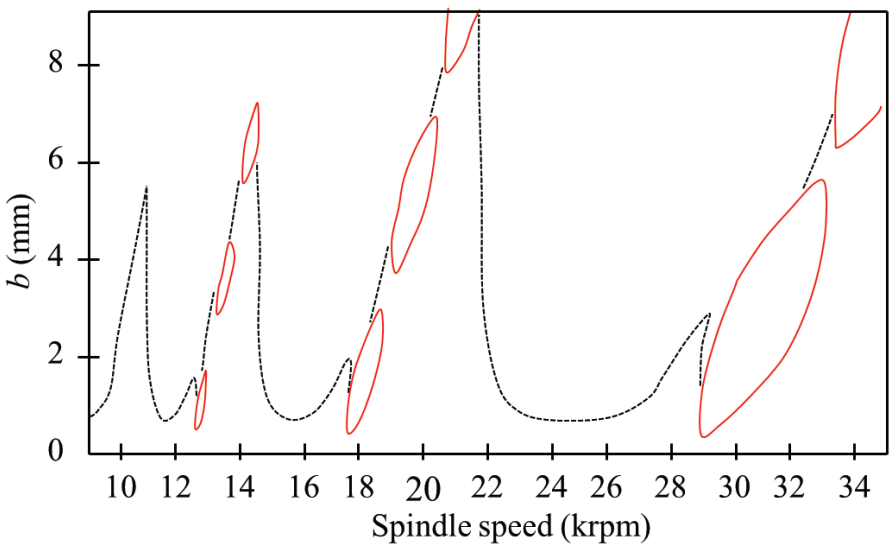

Fig. 4. Stability lobe diagram with secondary Hopf (dashed) and period-2 (solid) stability boundary obtained using the semi-discretization method [15].

The stability diagram obtained using the amplitude ratio stability metric is given in Fig. 5. The agreement between the stability diagrams is evident. It is observed that the amplitude ratio diagram predicts a similar stability boundary between stable and unstable spindle speed-axial depth of cut combinations. Additionally, the regions of period-2 instability are visible.

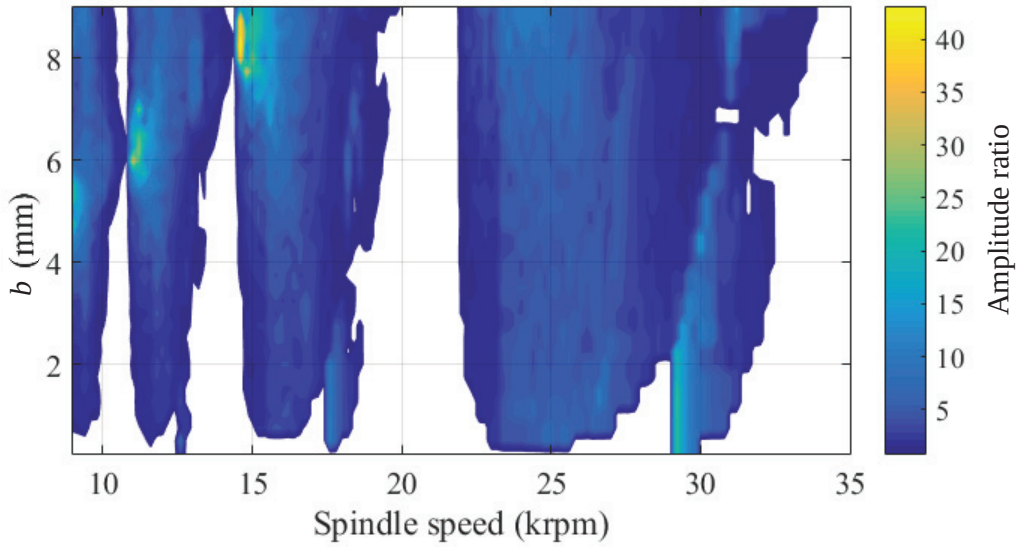

Fig. 5. Amplitude ratio diagram with secondary Hopf and period-2 stability boundary using time domain simulation.

4.2. Helix Angle Induced Islands of Instability

In [16] Insperger, Muñoa, Zatarain, and Peigné use the semi-discretization approach to show that unstable period-2 islands manifest on the milling stability diagram due to the helix angle of the cutting tool. In this numerical study a four flute, 20 mm diameter endmill with various helix angles was used in a down milling configuration. Flexibility in the milling system occurs on the workpiece side in the *y* direction using a flexure with the modal parameters provided in Table 2. The tool is considered quasi-rigid, relative to the flexure, in both the *x* (feed) and *y* directions. The radial immersion is 5% (i.e., 1 mm) and the cutting force coefficients in the tangential and radial directions are 804.3 MPa and 331 MPa, respectively.

Table 2. Modal parameters for the workpiece (flexure) measured using impact testing.

y (feed) direction		
f_n (Hz)	k (N/m)	ζ
319.375	2.16×10^7	0.0196

Milling stability diagrams were generated using the semi-discretization approach for tools of different helix angle. Insperger et al. define the helical pitch, p, as:

$$p = \frac{D\pi}{N \tan \eta} \tag{11}$$

where D is the tool diameter, N is the number of cutting teeth, and η is the helix angle. Milling stability diagrams, generated using the semi-discretization approach, for helical pitches of 100 mm, 50 mm, and 25 mm are given in Fig. 6. Rather than spindle speed, the horizontal axis is expressed as the ratio of the tooth passing frequency to the

natural frequency of the system providing a "normalized spindle speed." As noted by Insperger *et al.* the stability islands are separated by lines where the axial depth of cut is equal to the multiples of the helical pitch.

Fig. 7 shows the amplitude ratio diagram obtained using time domain simulation. The agreement between the two stability diagrams is evident. The amplitude ratio diagram predicts a similar stability limit between stable and unstable combinations of spindle speed and axial depth of cut. Additionally, the unstable islands of instability due to cutting tool helix angle are apparent.

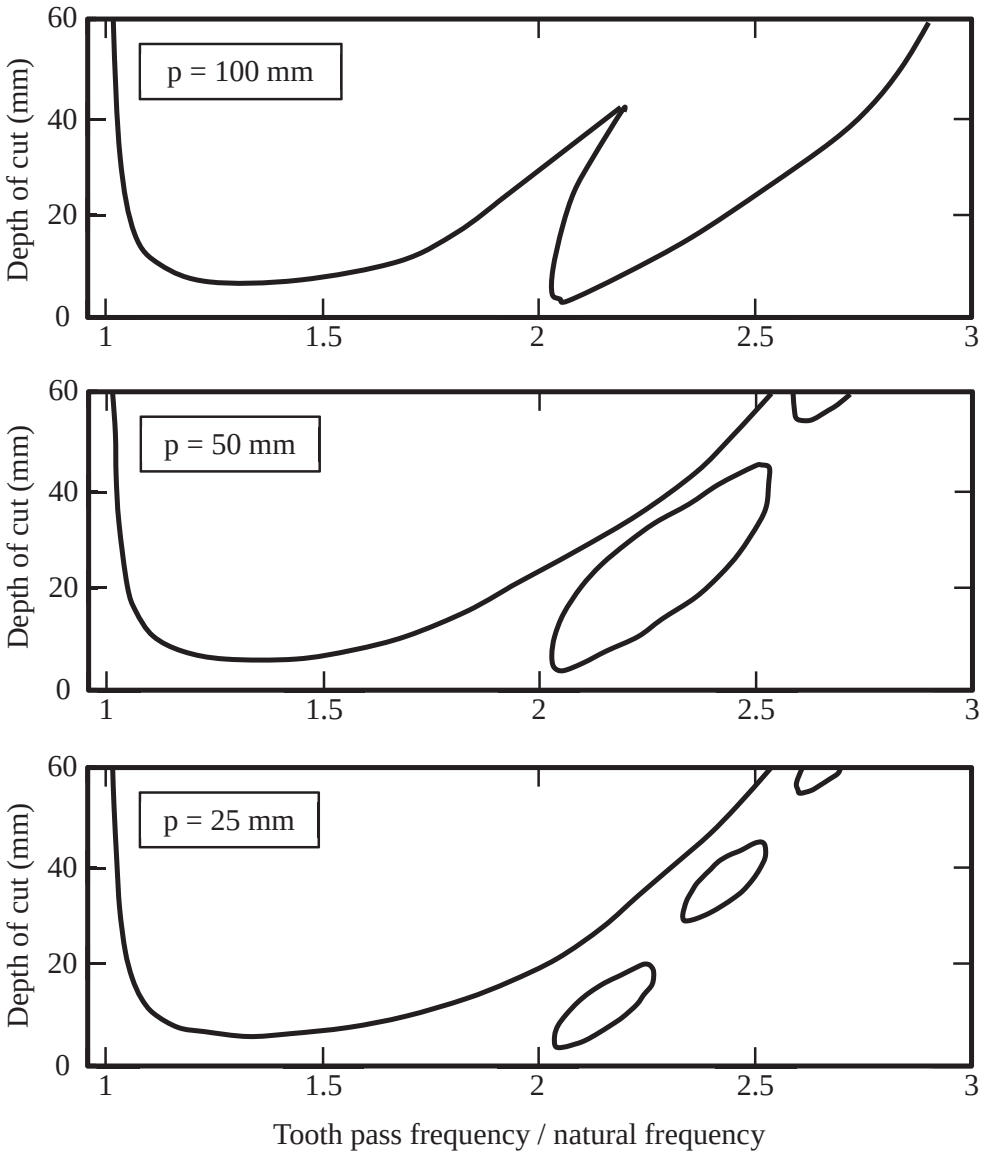

Fig. 6. Milling stability diagrams for different helical pitches using the semi-discretization method [16].

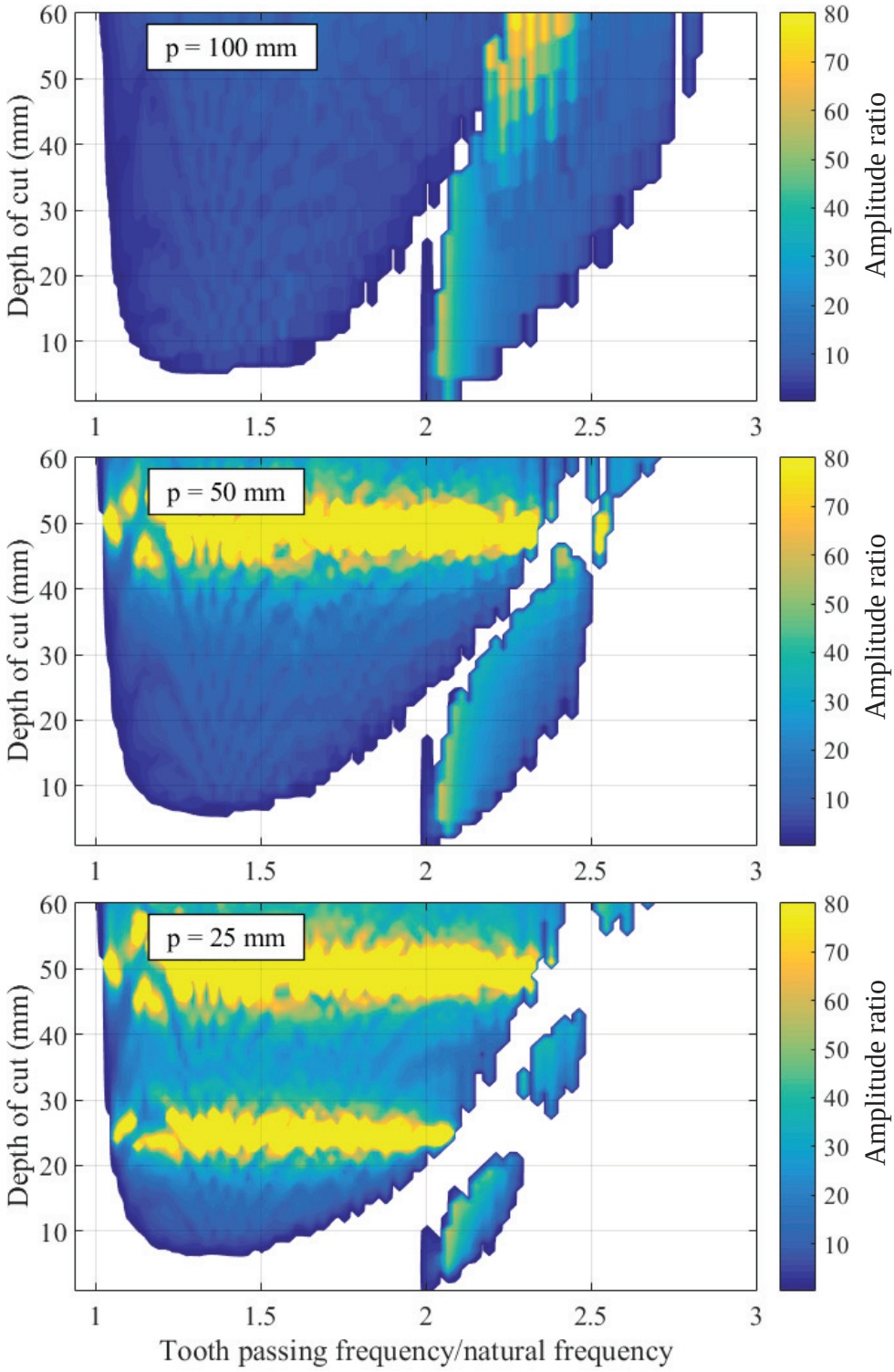

Fig. 7. Amplitude ratio diagram for different helical pitches using time domain simulation.

5. Conclusions

In this paper, the amplitude ratio stability metric was presented. The time domain simulation model was described, including the mechanistic force model and Eulerian integration approach, for solving the dynamic equations of motion. The suitability of the amplitude ratio was evaluated through comparison with independently published results which were obtained using the semi-discretization method. It was demonstrated that the amplitude ratio stability metric is suitable for evaluating the stability of milling operations simulated in the time domain. Additionally, the amplitude ratio provides a quantitative measure of the severity of chatter. It may be the case that a small chatter frequency component ($r_{amp} \ll 1$) results in sufficient workpiece dimensional accuracy and surface finish making it acceptable for some machine shop applications. However, as the amplitude ratio becomes larger chatter becomes increasingly severe and prohibitive.

References

[1] F.W. Taylor, The art of cutting metals, Scientific American, 63 (1907) 25942-25944.
[2] S. Tobias, W. Fishwick, Theory of regenerative machine tool chatter, The engineer, 205 (1958) 199-203.
[3] J. Tlusty, M. Polacek, The stability of machine tools against self-excited vibrations in machining, International research in production engineering, 1 (1963) 465-474.
[4] H.E. Merritt, Theory of self-excited machine-tool chatter: Contribution to machine-tool chatter research—, Journal of Manufacturing Science and Engineering, 87 (1965) 447-454.
[5] S. Smith, J. Tlusty, Efficient simulation programs for chatter in milling, CIRP Annals - Manufacturing Technology, 42 (1993) 463-466.
[6] M.L. Campomanes, Y. Altintas, An improved time domain simulation for dynamic milling at small radial immersions, Journal of Manufacturing Science and Engineering, 125 (2003) 416.
[7] A. Honeycutt, T. Schmitz, A new metric for automated stability identification in time domain milling simulation, Journal of Manufacturing Science and Engineering, 138/7 (2016) 074501.
[8] S. Smith, D. Dvorak, Tool path strategies for high speed milling aluminum workpieces with thin webs, Mechatronics, 8 (1998) 291-300.
[9] S. Smith, J. Tlusty, An overview of modeling and simulation of the milling process, Journal of engineering for industry, 113 (1991) 169-175.
[10] J. Tlusty, Manufacturing Processes and Equipment, Prentice Hall, 2000.
[11] J. Tlusty, F. Ismail, Basic non-linearity in machining chatter, CIRP Annals - Manufacturing Technology, 30 (1981) 299-304.
[12] M.A. Davies, B. Dutterer, J.R. Pratt, A.J. Schaut, J.B. Bryan, On the dynamics of high-speed milling with long, slender endmills, CIRP Annals - Manufacturing Technology, 47 (1998) 55-60.
[13] E. Budak, Y. Altintas, E. Armarego, Prediction of milling force coefficients from orthogonal cutting data, Journal of Manufacturing Science and Engineering, 118 (1996) 216-224.
[14] C.T. Tyler, T.L. Schmitz, Analytical process damping stability prediction, Journal of Manufacturing Processes, 15 (2013) 69-76.
[15] E. Govekar, J. Gradišek, M. Kalveram, T. Insperger, K. Weinert, G. Stépàn, I. Grabec, On stability and dynamics of milling at small radial immersion, CIRP Annals - Manufacturing Technology, 54 (2005) 357-362.
[16] T. Insperger, J. Munoa, M. Zatarain, G. Peigne, Unstable islands in the stability chart of milling processes due to the helix angle, in: CIRP 2nd International Conference on High Performance Cutting, Vancouver, Canada, 2006.